



Detection of O-glycosylated CA125 by using an electrochemical immunosensor for ovarian cancer diagnosis

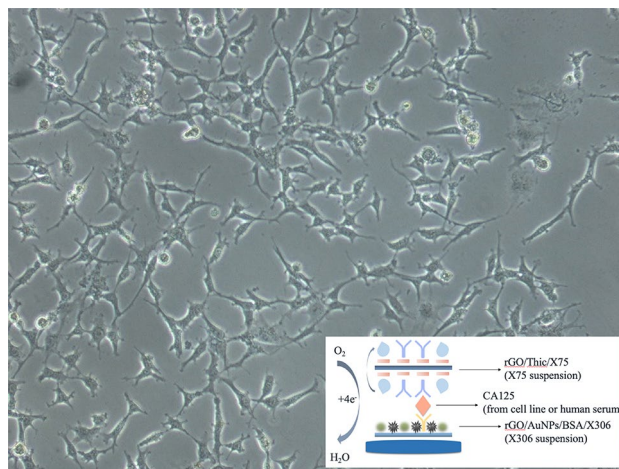
Fu-Ming Wang^{1,2,3,4} · Shih-Han Huang¹ · Chiou-Chung Yuan⁵ · Chi-Tai Yeh⁶ · Wei-Ling Chen¹ · Xing-Chun Wang¹ · Nattharika Runprapan¹ · Yueh-Ju Tsai⁷ · Ya-Lin Chuang⁵ · Chia-Hung Su⁸

Received: 11 April 2020 / Accepted: 1 September 2020 / Published online: 12 September 2020
© Springer Nature B.V. 2020

Abstract

Patients with ovarian cancer exhibit no clear symptoms. Ovarian cancer can be detected early only through internal diagnosis, ultrasound, and a carcinoma antigen 125 (CA125) tumor index test. More than 60% of patients have advanced ovarian cancer at diagnosis. The traditional chemical fluorescence immunoassay is used to measure CA125 levels; its lowest detection limit is only 35 U mL^{-1} , but it does not adequately demonstrate early symptoms. Moreover, endometriosis, pelvic cavity inflammation, and other gynecological diseases may increase CA125 levels. Therefore, a method for extracting CA125 information is urgently required for ovarian cancer diagnosis. This information can include the glycosylated state of CA125. In this study, a new ultrasensitive electrochemical immunosensor composed of reduced graphene oxide (rGO), gold nanoparticles, thionine chloride, bovine serum albumin, and two antibodies was developed. Through hydrogen peroxide reduction, the sensor can detect glycosylated CA125 from ovarian cancer cells and human blood serum by using differential pulse voltammetry. O_2 reacts with H^+ that the H^+ is formed from altered glycan core structures, producing a strong signal for malignancy detection. With the lowest detection limit of 4.10 pg mL^{-1} (127 nU mL^{-1}), the sensor can be used for early ovary cancer detection. Furthermore, the results of a clinical test in healthy individuals and patients demonstrated the high selectivity of the immunosensor, and the high-regression-curve rate obtained from human blood serum analysis could be used to distinguish ovarian cancer from other gynecological diseases. This is the first study employing an electrochemical immunosensor to define and identify ovarian cancer to achieve highly specific and accurate detection.

Graphic abstract



Keywords Ovarian cancer · Electrochemical · Sensor · CA125 · Serum · O-glycosylated

Extended author information available on the last page of the article

1 Introduction

Ovarian cancer, a gynecological cancer, is the most common in menopausal or postmenopausal women, particularly in women aged > 50 years. Because the initial symptoms of ovarian cancer are unclear or are similar to gastrointestinal symptoms, treatment can be delayed. According to clinical reports, in most cases, ovarian cancer is diagnosed at stage three or higher, and its prognosis is poor. The 5-year survival rate is < 20%. The most common type of ovarian cancer is ovarian epithelial cell carcinoma, accounting for up to 95% cases. Ovarian epithelial cell carcinoma has five subtypes, among which highly differentiated serous ovarian cancer is the most malignant. Currently, numerous tumor biomarkers are used to screen for ovarian cancer. The most commonly employed biomarker is carcinoma antigen 125 (CA125) or mucin 16. CA125 is a major tumor biomarker produced by mesothelial and epithelial ovarian tumors. Its concentration in body fluids varies among individuals. Clinically, a CA125 level of > 35 U mL⁻¹ is considered a preliminary indication of ovarian cancer. Currently, many detection and analysis methods, including radioimmunoassay [1], immune polymerase chain reaction assay [2], electrophoretic immunoassay [3], mass spectrometric immunoassay [4], and enzyme-linked immunosorbent assay (ELISA) [5], are used for ovarian cancer detection. However, these methods are less sensitive and time consuming and cannot be used to distinguish structural changes in CA125 because of pregnancy [6], endometriosis [7], reproductive age [8], and gynecological diseases [9, 10]; these changes may cause false-positive results.

Some studies have reported that differences in CA125 glycosylation (O- and N-glycans) can be employed to detect ovarian cancer in women; however, the actual sites of glycan attachment remain unknown [11, 12]. Rudd et al. demonstrated that in patients with ovarian cancer, the levels of core-fucosylated agalactosyl biantennary glycans incrementally increased, and that most bisecting bi-antennary and nonfucosylated glycans decreased compared with controls, indicating differences in CA125 N-glycan [13]. They reported that these differences in N-glycan segments are the increase in size, branching, and sialylation of structures. Moreover, through mass spectrometry, they found that CA125 O-glycan contained core 1 and 2 structures. Tsuboi and Fukuda reported that core 2 O-glycans may promote the growth of tumor cells and their survival for a longer duration in circulatory systems, leading to tumor metastasis [14]. Interestingly, Clausen et al. reported that N-glycosylation or O-glycosylation did not strongly influence the binding of anti-CA125 and monoclonal antibodies, and that the binding epitopes of these two antibodies

depended on the conformation and not on glycosylation, because a complete sperm protein, enterokinase, and agrin (SEA) domain was not required [15]. These findings revealed that protein glycosylation (especially O-glycans) provides crucial information for cancer diagnosis. However, currently, no universal method for the rapid and reliable identification of glycan structures is available [16]. Using a simple detection method for recognizing changes in glycosylation based on molecular characteristics is difficult. Moreover, CA125 may be a specific biomarker of ovarian cancer. Thus, a method for detecting the glycosylated state of CA125 is urgently required.

In addition, glassy carbon has been used as a working electrode in electrochemical reaction for the detections of Tramadol [17], Viagra [18], energy conversion [19].

In this study, a novel electrochemical immunosensor for detecting O-glycosylated CA125 was developed. The immunosensor was composed of reduced graphene oxide (rGO), gold nanoparticles, thionine chloride (Thic), bovine serum albumin (BSA), and two antibodies. The rGO is a substrate for providing electric conductivity and the gold nanoparticles can significantly improve the electric conductivity. Thic provides two functions in this study including the dissociated chlorine ion and connecting the antibody. BSA is a protein and used to block some remain active sites after the antibody is reacted. The ES-2 cells are employed for electrochemical immunoanalytical detection and serum analysis.

2 Experimental

2.1 Materials

rGO was purchased from Cheap Tubes company (VT, USA). Thic, glutaraldehyde, chitosan, phosphate-buffered saline (PBS, 0.1M, pH 7.4), hydrogen peroxide, and anti-CA125 X75 and X306 antibodies were obtained from UNI-ONWARD (New Taipei City, Taiwan). Hydrogen tetrachloroaurate hydrate (HAuCl₄·H₂O, 99.9%) and sodium borohydride (NaBH₄) were obtained from Echo Chemical Co., Ltd. (Taipei, Taiwan). The clonality of X75 (M 11-like) and X306 (OC 125-like) anti CA125 antibodies was monoclonal and hosted by a mouse.

2.2 Instruments

All electrochemical measurements were performed using a multichannel potentiostat (VMP3, Bio-Logic Science Instruments). A glassy carbon (GC) electrode was used as the working electrode, with Ag/AgCl and a platinum wire acting as reference and counter electrodes, respectively. Optical microscopy (OM, MXK600, Microtech Optical Co.) was employed to study cell cultures. A pH meter (INLAB

ROUTINE, Mettler Toledo Co.) was employed for analyzing the H^+ concentration. The phase composition was studied using an X-ray diffractometer (XRD) (D₂ Phaser, Bruker, Karlsruhe, Germany) with a range from 10° to 60°, increments of 0.5°, and scanning rate of 5°/min. The chemical analysis is characterized using an attenuated total reflection FTIR (ATR-FTIR) analyzer in the frequency range of 4000–400 cm^{-1} (FT/IR-6700, JASCO, Japan). The morphologies are detected through scanning electron microscopy (SEM) by using a LEO-1530 microscope.

2.3 Synthesis of Au nanoparticles

Au nanoparticles were synthesized, as reported in [20]. First, 50 μL aqueous solution of 10 mM $H AuCl_4$ was mixed with 3 mL of 0.2 wt% chitosan (in an aqueous solution of 1% acetic acid). The mixture was stirred for 30 min. Subsequently, 50 μL of 0.1 M $NaBH_4$ was added to the mixture, and the solution was stirred for 90 min. The resulting solution of Au nanoparticles was stored at 4 °C. Figure 1 illustrates

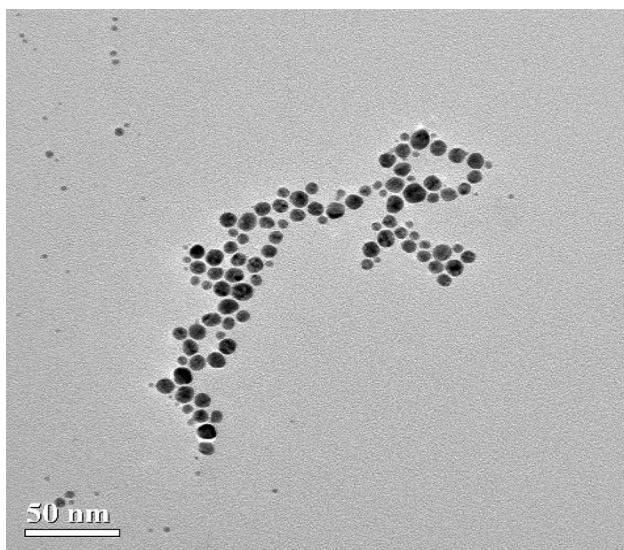


Fig. 1 Transmission electron microscopy image of Au nanoparticles

that nanoparticle diameters obtained through transmission electron microscopy were 9–11 nm.

2.4 Preparation of rGO/Thic/X75 antibody suspension solution

In 60 μL PBS at pH 7.4, 1.2 mg rGO was dispersed; subsequently, 1 mM Thic was added. The resulting mixture was stirred for 48 h at 37 °C. After stirring, 2.5% glutaraldehyde was added, and the solution was stirred for 1 h at room temperature. Thereafter, 3.38 μL X75 was added to the solution. The mixture was incubated at room temperature and stirred for 1 h. The resulting (rGO/Thic/X75) suspension solution was stored at 4 °C before use.

In order to analyze the chemical and physical properties of rGO/Thic/X75 composite, the SEM, XRD, and ATR-FTIR are adopted. Figure 2a displays the rGO/Thic/X75 composite is a flake-like morphology, which is the original morphology of rGO, indicating the X75 does not affect rGO. Figure 2b shows a (002) phase of rGO and cannot find other crystal phase is formed on the rGO/Thic/X75 composite. Figure 2c shows several absorptions on spectrum such as the peaks at 2924 and 2854 cm^{-1} mark the stretch vibrations of $-C-H(CH_2)$ and $-C-H(CH_3)$ groups of X75 as well as the peaks at 1586 and 1157 cm^{-1} are $-C=C-$ and $-C-OH$ from rGO.

2.5 Preparation of rGO/X306 antibody suspension solution and

In PBS at pH 7.4, 1.2 mg rGO was dispersed, and 1 μL X306 was added, and the resulting solution was incubated for 1 h. Subsequently, 1 wt% BSA was added to the solution of Au nanoparticles. BSA was used to block the remaining active sites and to prevent nonspecific bonding. Thereafter, various concentrations of the CA125 antigen were added, and the mixture was incubated for another 1 h. The resulting rGO/X306 suspension solution was stored at 4 °C before use.

In order to analyze the chemical and physical properties of rGO/X306 composite, the SEM, XRD, and ATR-FTIR

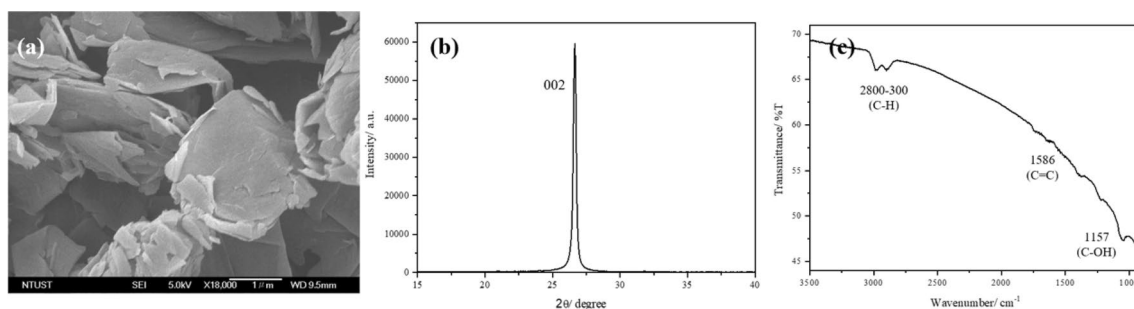


Fig. 2 The analysis of **a** SEM, **b** XRD, **c** ATR-FTIR of rGO/Thic/X75 composite

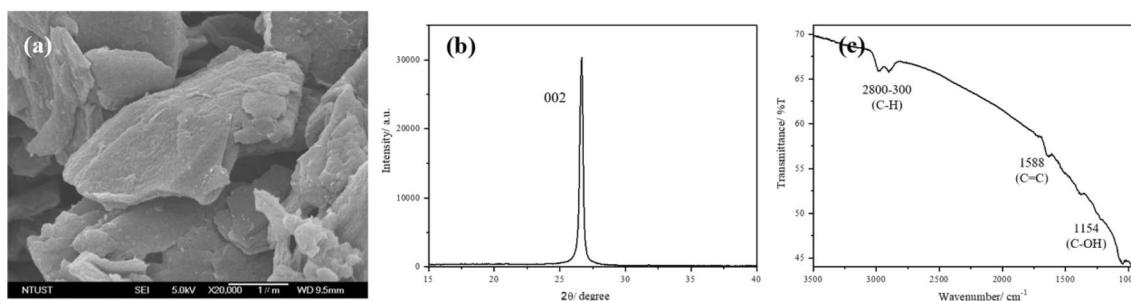


Fig. 3 The analysis of **a** SEM, **b** XRD, **c** ATR-FTIR of rGO/X306 composite

are adopted. Figure 3a displays the rGO/X306 composite is a flake-like morphology, which is the original morphology of rGO. However, the surface of rGO covers a film on rGO/X306 composite, which is not like rGO/Thic/X75 composite, indicating the X306 has a significant reaction with rGO. Figure 3b shows a (002) phase of rGO and cannot find other crystal phase is formed on the rGO/Thic/X75 composite. Figure 3c shows several absorptions on spectrum such as the peaks at 2921 and 2856 cm^{-1} mark the stretch vibrations of $-\text{C}-\text{H}(\text{CH}_2)$ and $-\text{C}-\text{H}(\text{CH}_3)$ groups of X75 as well as the peaks at 1588 and 1154 cm^{-1} are $-\text{C}=\text{C}-$ and $-\text{C}-\text{OH}$ from rGO.

2.6 CA125 collection from cell lines and human blood serum

Hey A8 and ES-2 cell lines were provided by American Type Culture Collection. The cell lines were stored in McCoy 5A medium (Gibco, Life Technologies, USA) supplemented with 10% fetal bovine serum under standard conditions. N-glycan was extracted from the serum through peptide-N-glycosidase F (Mannheim, Germany). O-glycans were released and extracted after N-glycans were released from SDS-gel blocks in order to collect the O-glycosylated CA125 [13]. Human blood samples were collected from four patients (two with ovarian cancer, one with endometriosis, and one with germ cell tumor) who were treated at Taipei Medical University Shuang Ho Hospital. The blood samples were immediately centrifuged after collection to obtain the serum. Within 1 h of obtaining the serum, it was analyzed using ELISA and the electrochemical immunosensor.

2.7 Western blotting

Western blotting was performed using the standard method. The membrane was incubated with the primary antibody X306.

2.8 Serum collection

The serum samples were obtained from Taipei Medical University-Shuang Ho Hospital and Cheng Hsin General Hospital, and this study was conducted the guidelines of the Cheng Hsin General Hospital Permission of Clinical Trial (CHGH) and with the approval of Taipei Medical University Joint Institutional Review Board (TMU-JIRM). All serum-related experiments were conducted in accordance with CHGH and TMU-JIRM guidelines, and all experimental protocols were approved (No. 622-106A-30, dated June 21, 2018 and No. N201706039, dated July 14, 2017).

2.9 Fabrication of the electrochemical immunosensor and analysis

Figure 4 illustrates the construction of the electrochemical immunosensor. Different concentrations of O-glycosylated CA125 extracted from ES-2 cells were first added to 1 g rGO/Thic/X75 antibody suspension solution, and the solution was stirred for 1 h at 4 °C. By contrast, 1 g rGO/X306 antibody suspension solution was added to the rGO/Thic/X75/O-glycosylated CA125 solution. The sandwich electrochemical immunosensor product (rGO/Thic/X75/O-glycosylated CA125/X306/rGO) was stirred for another

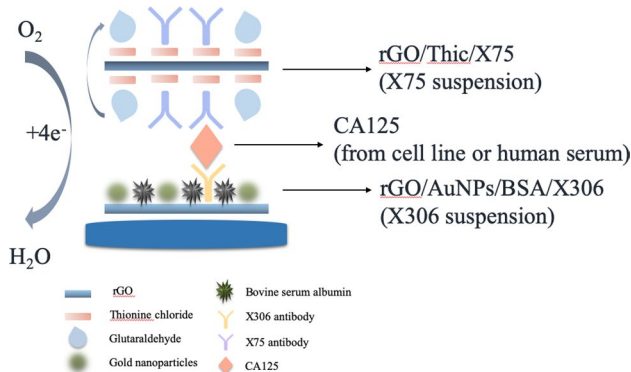


Fig. 4 Electrochemical immunosensor

1 h at 4 °C. Before electrochemical measurement, 0.1M H₂O₂ was added for O-glycosylated CA125 detection. The GC, platinum wire, and Ag/AgCl electrodes are separately immersed into above mixing solution (0.1M H₂O₂ in rGO/Thic/X75/O-glycosylated CA125/X306/rGO solution) for electrochemical measurements. Differential pulse voltammetry (DPV) with a pulse amplitude and width of 50 mV and 50 ms, respectively, was employed. An electrochemical window was set from an open circuit voltage to -0.7 V for ES-2 cells and -1.2 V for serum measurements.

3 Results and discussion

Figure 5a and 5b present the OM images of ES-2 spheroidal cell cultures obtained after different incubation times. The incubated cells were nearly spheroidal on the first day, and the cell diameter was approximately 25 μ m. After 3 days of incubation, the cells exhibited a narrow shape, indicating that they were malignant. Figure 5a and 5b illustrate similar behavior for Hey-A8 spheroidal cell cultures, indicating that the incubation time for Hey-A8 and ES-2 cell lines was sufficient for CA125 collection.

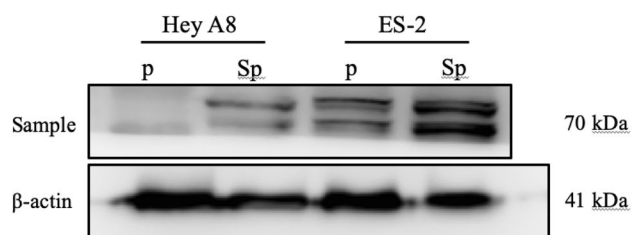


Fig. 6 Protein levels in Hey-A8 and ES-2 cells in parental (p) and spheroids (Sp) assessed through Western blotting

Figure 6 illustrates that CA125 obtained from ES-2 spheroidal cells was primarily responsive to cisplatin, and that ES-2 spheroidal cells with X75 antibodies were strongly active. Unlike the unclear images of Hey-A8 and ES-2 parental cells, the images of ES-2 spheroidal cells demonstrated that the cells were sensitive. Therefore, ES-2 spheroidal cells were selected to study O-glycosylated CA125 production.

Figure 7 presents the plot of the DPV response of the electrochemical immunosensor as a function of different concentrations of O-glycosylated CA125. Two reactions

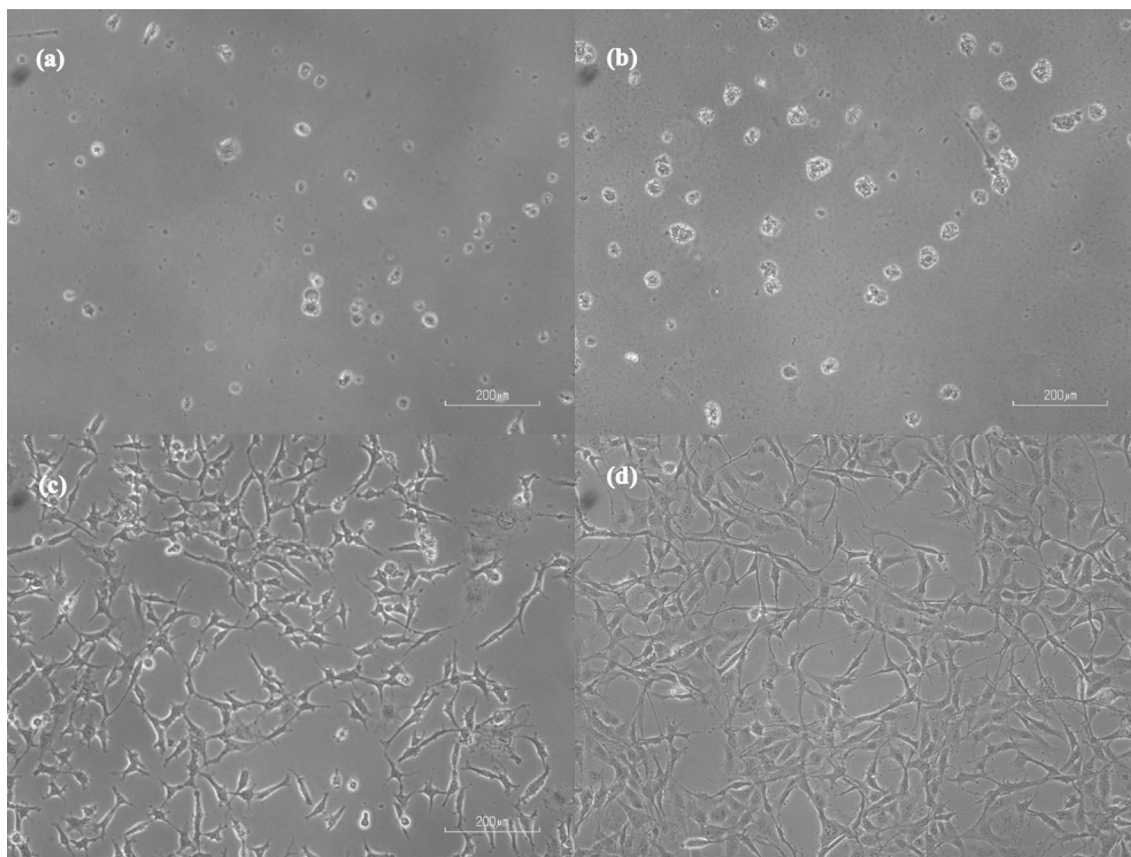
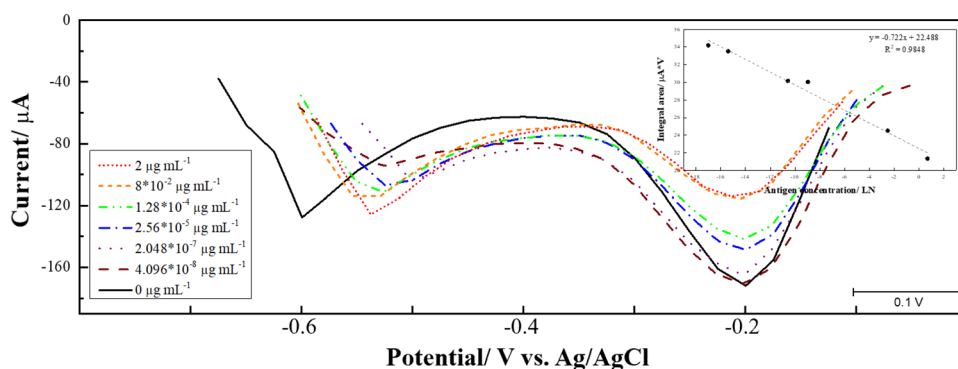


Fig. 5 OM images of ES-2 (left) and Hey-A8 (right) spheroids cell culture obtained **a** and **b** on day 1 and **c** and **d** after 3 days of incubation

Fig. 7 DPV response of the electrochemical immunosensor for the varying concentrations of O-glycosylated CA125 collected from ES-2 spheroidal cells



occurred at -0.2 and -0.6 V. According to the literature, the first reaction (-0.2 V) was the oxygen reduction reaction (ORR), involving H_2O_2 decomposition. ORR is presented in Eqs. (1) and (2). The second reaction (-0.6 V) was the direct reduction of H_2O_2 and is presented in Eq. (3) [21].



With an increase in the concentration of O-glycosylated CA125, the reaction current intensity of the ORR decreased, indicating that O-glycosylated CA125 reacted with antibodies and blocked any reaction at the electrode surface. However, a change in the concentration of O-glycosylated CA125 did not strongly affect the direct reduction of H_2O_2 . This result revealed that O-glycans can release H^+ from its carboxyl group, and H^+ in combination with O_2 may exhibit a remarkable effect and gradually decrease the rate of the reaction presented in Eq. (2). In addition, unreacted residual H_2O_2 was then independently reduced and did not react with CA125. A study reported that a typical change in O-glycosylated CA125 is the loss of branched core-2 or core-4 O-glycans and the overexpression of simple or truncated core-1 O-glycans [22]. These changes in glycan core structures can lead to some reactions with O_2 and produce a critical signal that can be used for detecting malignancy. O-glycosylation is the attachment of a sugar molecule to an oxygen atom [23] or a OH group [16] of hydroxy amino acids in a protein. Therefore, the proton present in the OH group of O-glycosylated CA125 was used for reduction with O_2 to an ORR reaction of Eq. (2).

The response current was saturated at the highest concentration ($2 \mu\text{g mL}^{-1}$, approximately 0.05 U mL^{-1}) of O-glycosylated CA125 occupation (Fig. 7). The lowest detection limit of the immunosensor was 4.10 pg mL^{-1} (approximately 127 nU mL^{-1}), and the regression rate of the calibration

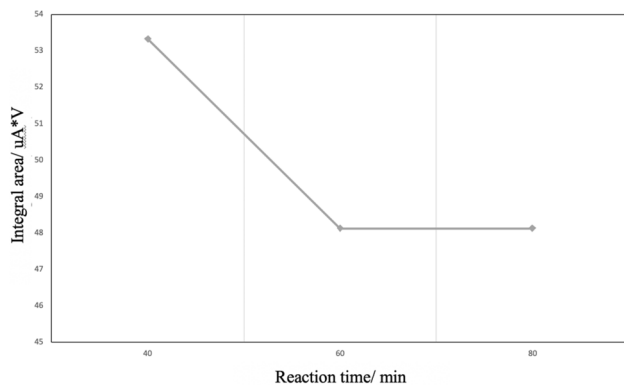
curve was 0.98. Compared with sensors such as Au@ Co_3O_4 nanosheets (lowest detection limit = 250 ng mL^{-1}) [24], multiwalled carbon nanotubes (lowest detection limit = 1.13 mU mL^{-1}) [25], Prussian blue-platinum nanoparticles (lowest detection limit = 4.4 mU mL^{-1}) [26], a three-dimensional gold nanoelectrode ensemble (lowest detection limit = 500 mU mL^{-1}) [27], ZnO nanorod-Au nanoparticle nanohybrids (lowest detection limit = $2.5 \mu\text{g mL}^{-1}$) [28], and a gold electrode with mercaptopropionic acid-silica-CdSe quantum dots (lowest detection limit = 1.6 mU mL^{-1}) [29] reported in other studies on normal CA125, the immunosensor developed in this study exhibited excellent detection performance and could be used to measure minute CA125 concentrations present in samples. According to the Table 1, this new electrochemical immunosensor shows the best performance than the others.

In addition, the response time and the stability of this electrochemical immunosensor has been evaluated. According to the result in Fig. 8, the reaction of the sandwich product (rGO/Thic/X75/O-glycosylated CA125/X306/rGO) can be totally completed within 60 min in accordance with the highest concentration ($2 \mu\text{g mL}^{-1}$, 0.05 U mL^{-1}) of O-glycosylated CA125 in Fig. 7 and shows no further reaction. This information indicates that this electrochemical immunosensor is eligible for fast screen detection with high discrimination.

Figure 9 illustrates the DPV response of the electrochemical immunosensor to serum collected from the four patients. According to the data of current clinical analyses, patients A and B had stage-four ovarian cancer; their CA125 levels were 233 and 66.4 U mL^{-1} , respectively, according to the traditional ELISA analysis. Patients C and D had endometriosis and germ cell tumor, respectively, and their CA125 levels were 22.2 and 13.3 U mL^{-1} , respectively, according to the traditional ELISA analysis. The serum obtained from patients C and D was compared with that obtained from patients A and B to confirm the specificity and reproducibility of the electrochemical immunosensor. For the serum obtained from patients A and B, the regression rate of calibration curves was 0.95 and 0.87, respectively (Fig. 9a and

Table 1 The comparisons of electrochemical immunosensor for ovarian cancer detection

Method	Detection limit	Commercial antigen	Cell line or serum	Reference
Au@Co ₃ O ₄ nanosheets	250 ng mL ⁻¹	V	X	[24]
Multiwalled carbon nanotubes	1.13 mU mL ⁻¹	V	X	[25]
Prussian blue-platinum nanoparticles	4.4 mU mL ⁻¹	V	X	[26]
Gold nanoelectrode ensemble	500 mU mL ⁻¹	V	X	[27]
ZnO nanorod-Au nanoparticle nanohybrids	2.5 μg mL ⁻¹	V	X	[28]
Mercaptopropionic acid–silica–CdSe quantum dots	1.6 mU mL ⁻¹	V	X	[29]
rGO for O-glycosylated CA125	4.10 pg mL ⁻¹ 127 nU mL ⁻¹	V	V	Our work

**Fig. 8** The response time and the stability of the electrochemical immunosensor with the maximum concentration of O-glycosylated CA125 in Fig. 7

9b). This finding revealed that the electrochemical immunosensor could detect O-glycosylated CA125 in real samples with high accuracy. The two curves were different according to the electrochemical tendency. Figure 9a illustrates a direct and broad ORR of O-glycosylated CA125; the current response gradually decreased with an increase in O-glycosylated CA125 levels. However, Fig. 9b reveals a narrow ORR of O-glycosylated CA125, and the peak behavior became gentle without mountain peak. This result is considerably different from that presented in Fig. 9a. Several studies have reported that the altered glycosylation biomarkers produced in cancers can exhibit glycosylation changes as their hallmarks [30, 31], such as high sialylation, branching, and outer arm fucosylation. This phenomenon may indicate that O-glycosylated CA125 obtained from different patients exhibited structural antigenic complexity with possible changes in molecular weights or structures. Thus, the ORR of CA125 can be employed to distinguish small changes in CA125 glycosylation for patients A and B. Moreover, the calibration curves (Fig. 9c and 9d) demonstrated that the regression rate was unreliable, which confirmed the specificity and reproducibility of the electrochemical immunosensor. In addition, the pH value of the serum solution acquired

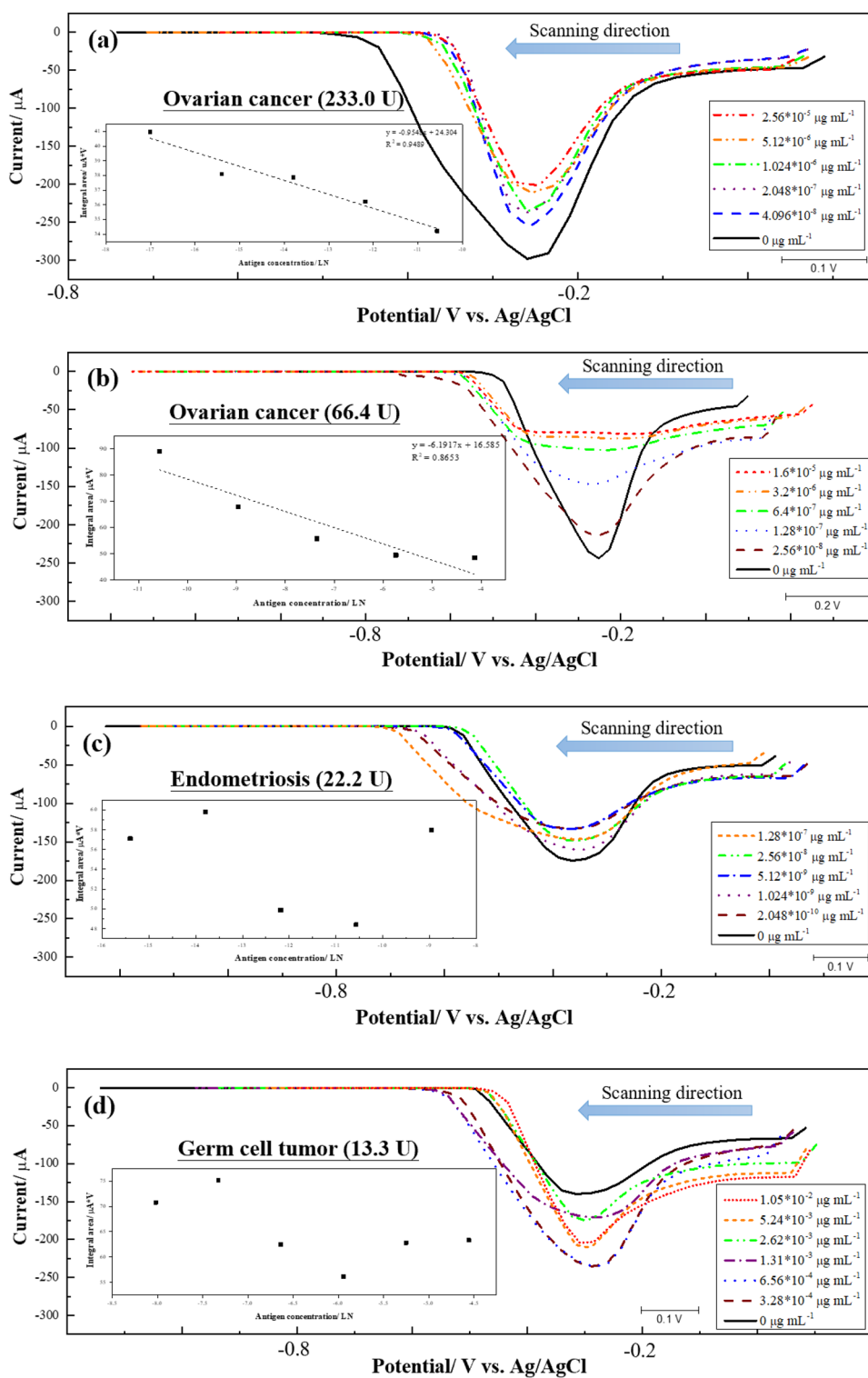
from patients A and B was measured, and the serum acquired from patients A exhibited lower pH (pH = 4.1) than that acquired from patient B (pH = 5.2), demonstrating the serum from patient A released many H⁺ for the ORR. By contrast, the pH of serum solution acquired from patients C and D was high (pH = 6.8).

Figure 10 illustrates the DPV response of the electrochemical immunosensor for serum obtained from a healthy human. The analysis result revealed no regression. The electrochemical immunosensor did not detect O-glycosylated CA125 in endometriosis, germ cell tumor, and healthy cases. However, typical changes and overexpression in O-glycosylation occurring in healthy individuals may not be similar to those occurring in patients with ovarian cancer. Thus, aberrant O-glycosylation is an inherent and specific property of cancer cells, which potentially helps in differentiating cancer from benign conditions and thus improves assay specificity. In addition, the pH of serum solution acquired from healthy human is slightly higher (pH = 7.4) than patients C and D, representing a normal serum sample. According to the results, (1) the mechanism of O₂ reacting with the different glycan core structures of O-glycosylated CA125 and (2) the difference between O-glycosylated CA125 obtained from patients A and B must be further investigated.

4 Conclusion

An electrochemical immunosensor, which can be used to detect the changes in the glycan core structure of CA125, was fabricated using rGO. This immunosensor can be used to sensitively distinguish among the serum obtained from patients with ovarian cancer, patients with other gynecological diseases, and healthy patients. Further investigation on the immunosensor is required, such as an independent proteomic analysis; however, these results provided valuable information for ovarian cancer detection.

Fig. 9 DPV response of the electrochemical immunosensor for patients **a** A, **b** B, **c** C, and **d** D



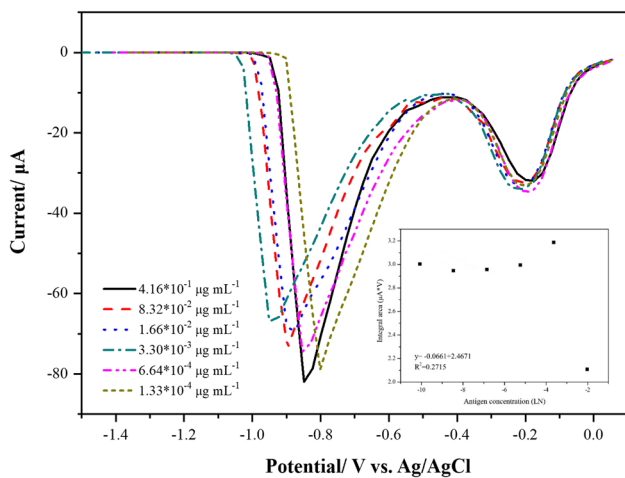


Fig. 10 DPV response of the electrochemical immunosensor for a healthy human

Acknowledgements The author is grateful for the financial support from the National Taiwan University of Science and Technology—Taipei Medical University Joint Research Program and the southern wisdom biomedical industry settlement plan of Southern Taiwan Science Park Bureau, the Ministry of Science and Technology (MOST) of Taiwan, R.O.C, Under Grant Numbers NTUST-TMU-No. 104-04, 106-04, and AZ-05-04-10-108.


References

- Goldsmith SJ et al (1975) Radioimmunoassay: review of basic principles. *Semin Nucl Med* 5:125–152. [https://doi.org/10.1016/S0001-2998\(75\)80028-6](https://doi.org/10.1016/S0001-2998(75)80028-6)
- Saito K et al (1999) Detection of human serum tumor necrosis factor- α in healthy donors, using a highly sensitive immuno-PCR assay. *Clin Chem* 45:665–669
- Moser AC et al (2008) Capillary electrophoresis-based immunoassays: principles and quantitative applications. *Electrophoresis* 29:3279–3295. <https://doi.org/10.1002/elps.200700871>
- Hu S et al (2007) Detection of multiple proteins on one spot laser ablation inductively coupled plasma mass spectrometry and application to immuno-microarray with element-tagged antibodies. *Anal Chem* 79:923–929. <https://doi.org/10.1021/ac061269p>
- Aebersold R et al (2003) Mass-spectrometric exploration of proteome structure and function. *Nature* 442:198–207. <https://doi.org/10.1038/nature19949>
- Shehata NAA et al (2018) Doppler and biochemical assessment for the prediction of early pregnancy outcome in patients experiencing threatened spontaneous abortion. *Int J Gynecol Obstet* 143:150–155. <https://doi.org/10.1002/ijgo.12631>
- Zheng R et al (2018) Predisposing factors for predicting the therapeutic response of adenomyosis after uterine artery embolization: serum CA125 levels and accompanying endometriosis. *Diagn Interv Radiol* 24:364–371. <https://doi.org/10.5152/dir.2018.17497>
- Socolov R et al (2017) An update on the biological markers of endometriosis. *Minerva Ginecol* 69:462–467. <https://doi.org/10.23736/S0026-4784.17.04046-1>
- Neriishi K et al (2018) Long-term dienogest administration in patients with symptomatic adenomyosis. *J Obstet Gynaecol Res* 44:1439–1444. <https://doi.org/10.1111/jog.13674>
- Zhao J et al (2018) Serum CA125 in combination with ferritin improves diagnostic accuracy for epithelial ovarian cancer. *Br J Biomed Sci* 75:66–70. <https://doi.org/10.1080/09674845.2017.1394051>
- Yin BW et al (2001) Molecular cloning of the CA125 ovarian cancer antigen: identification as a new mucin, MUC16. *J Biol Chem* 276:27371–27375. <https://doi.org/10.1074/jbc.M103554200>
- Wong NK et al (2003) Characterization of the oligosaccharides associated with the human ovarian tumor marker CA125. *J Biol Chem* 278:28619–28634. <https://doi.org/10.1074/jbc.M302741200>
- Saldova R et al (2013) Exploring the glycosylation of serum CA125. *Int J Mol Sci* 14:15636–15654. <https://doi.org/10.3390/ijms140815636>
- Tsuboi S et al (2012) Two opposing roles of O-glycans in tumor metastasis. *Trends Mol Med* 18:224–232. <https://doi.org/10.3390/ijms140815636>
- Marcos-Silva L et al (2014) Characterization of binding epitopes of CA125 monoclonal antibodies. *J Proteome Res* 13:3349–3359. <https://doi.org/10.1021/pr500215g>
- Marino K et al (2010) A systematic approach to protein glycosylation analysis: a path through the maze. *Nat Chem Biol* 6:713–723. <https://doi.org/10.1038/nchembio.437>
- Atta NF et al (2012) Monodispersed gold nanoparticles decorated carbon nanotubes as an enhanced sensing platform for nanomolar detection of tramadol. *Electroanalysis* 24:2135–2146. <https://doi.org/10.1002/elan.201200344>
- Farphali RA et al (2015) Gold nanoparticles-modified screen-printed carbon electrode for voltammetric determination of sildenafil citrate (Viagra) in pure form, biological and pharmaceutical formulations. *Int J Electrochem Sci* 10:1494–1505
- Galal A et al (2007) 2007 Hybrid organic/inorganic films of conducting polymers modified with phthalocyanines. I—film preparation and voltammetric studies. *J Solid State Electr* 11:521–530. <https://doi.org/10.1007/s10008-006-0189-9>
- Guo Z et al (2013) Multiplex electrochemiluminescence immunoassay of two tumors using multicolor quantum dots as labels and graphene as conducting bridge. *Biosens Bioelectron* 44:101–107. <https://doi.org/10.1016/j.bios.2013.01.025>
- Patra S et al (2009) Electrochemical reduction of hydrogen peroxide on stainless steel. *J Chem Sci* 121:675–683. <https://doi.org/10.1007/s12039-009-0081-0>
- Chen K et al (2013) Microarray glycoprofiling of CA125 improves differential diagnosis of ovarian cancer. *J Proteome Res* 12:1408–1418. <https://doi.org/10.1021/pr3010474>
- Van den Steen P et al (1998) Concepts and principles of O-linked glycosylation. *Crit Rev Biochem Mol Biol* 33:151–208. <https://doi.org/10.1080/10409239891204198>
- Ren X et al (2015) Ultrasensitive immunoassay for CA125 detection using acid site compound as signal and enhancer. *Talanta* 144:535–541. <https://doi.org/10.1016/j.talanta.2015.06.086>
- Paul KB et al (2017) Surface plasmon resonance as a tool for investigation of non-covalent nanoparticle interactions in heterogeneous self-assembly & disassembly systems. *Biosens Bioelectron* 88:144–152. <https://doi.org/10.1016/j.bios.2016.09.042>
- Zheng Y et al (2017) A nanocomposite containing prussian blue, platinum nanoparticles and polyaniline for multi-amplification of the signal of voltammetric immunosensors: highly sensitive detection of carcinoma antigen 125. *Microchim Acta* 184:4269–4277. <https://doi.org/10.1007/s00604-017-2470-2>
- Viswanathan S et al (2012) Molecular imprinted nanoelectrodes for ultra sensitive detection of ovarian cancer marker. *Biosens Bioelectron* 33:179–183. <https://doi.org/10.1016/j.bios.2011.12.049>
- Gasparotto G et al (2017) Electrochemical immunosensor based on ZnO nanorods-Au nanoparticles nanohybrids for ovarian cancer antigen CA-125 detection. *Mater Sci Eng, C* 76:1240–1247. <https://doi.org/10.1016/j.msec.2017.02.031>

29. Johari-Ahar M et al (2015) A ultra-sensitive impedimetric immunosensor for detection of the serum oncomarker CA-125 in ovarian cancer patients. *Nanoscale* 7:3768–3779. <https://doi.org/10.1039/C4NR06687A>
30. Munkley J et al (2016) Hallmarks of glycosylation in cancer. *Oncotarget* 7:35478–35489. <https://doi.org/10.18632/oncotarget.8155>
31. Pinho SS et al (2015) Glycosylation in cancer: mechanism and clinical implications. *Nat Rev Cancer* 15:540–555. <https://doi.org/10.1038/nrc3982>

Publisher's Note Springer Nature remains neutral with regard to jurisdictional claims in published maps and institutional affiliations.

Affiliations

Fu-Ming Wang^{1,2,3,4}  · Shih-Han Huang¹ · Chiou-Chung Yuan⁵ · Chi-Tai Yeh⁶ · Wei-Ling Chen¹ · Xing-Chun Wang¹ · Nattharika Runprapan¹ · Yueh-Ju Tsai⁷ · Ya-Lin Chuang⁵ · Chia-Hung Su⁸

✉ Fu-Ming Wang
mccabe@mail.ntust.edu.tw

✉ Chiou-Chung Yuan
ccyuan62@gmail.com

¹ Graduate Institute of Applied Science and Technology, National Taiwan University of Science and Technology, Taipei, Taiwan

² Sustainable Energy Center, National Taiwan University of Science and Technology, IB 606, 43 Keelung Road, Section 4, Taipei 106, Taiwan, R.O.C.

³ Department of Chemical Engineering, Chung Yuan Christian University, Taoyuan, Taiwan

⁴ R&D Center for Membrane Technology, Chung Yuan Christian University, Taoyuan, Taiwan

⁵ Department of Obstetrics and Gynecology, Cheng Hsin General Hospital, Taipei, Taiwan

⁶ Department of Medical Research and Education, Taipei Medical University-Shuang Ho Hospital, Taipei, Taiwan

⁷ Department of Obstetrics and Gynecology, Taipei Medical University-Shuang Ho Hospital, Taipei, Taiwan

⁸ Graduate School of Biochemical Engineering, Ming Chi University of Technology, Taipei, Taiwan